ELSEVIER

International Journal of Heat and Fluid Flow 19 (1998) 115–124

International Journal of HEAT AND FLUID FLOW

Enhancement of impinging jet heat transfer by making use of mechano–fluid interactive flow oscillation

Y. Haneda [a], Y. Tsuchiya [b], K. Nakabe [c], K. Suzuki [c,*]

[a] *Department of Mechanical Engineering, Nagano National College of Technology, 716 Tokuma, Nagano 381, Japan*
[b] *Department of Mechanical Systems Engineering, Shinshu University, 500 Wakasato, Nagano 380, Japan*
[c] *Department of Mechanical Engineering, Kyoto University, Kyoto 606-01, Japan*

Received 5 July 1997; accepted 25 October 1997

Abstract

Heat transfer and fluid flow measurements were conducted for a two-dimensional impinging jet in which a cylinder suspended with springs at both its ends was inserted. The jet Reynolds number was set at about 10,000 and the target plate was mounted at two different distances from the jet exit of 3 and 5 times the jet slot width. Insertion of a rigidly suspended cylinder deteriorates the heat transfer around the stagnation region while it effectively enhances heat transfer outside the stagnation region. This is further improved by suspending the cylinder with springs. The maximum Nusselt number attained around the stagnation point was augmented by about 20% compared to the one for normal impinging jet without the insertion of a cylinder. A cross-stream oscillatory motion of the cylinder was produced perpendicular to its axis due to the interaction between the vortex shedding from the cylinder and the cylinder-spring mechanical oscillation system. Intensive periodical velocity and pressure fluctuations were induced in the wake of the cylinder. The fluctuating flow pattern appearing near the geometrical center of the target plate was estimated to be a swing-type one.

Keywords: Jet impingement; Oscillating cylinder; Heat transfer enhancement; Nusselt number; Velocity fluctuation; Flow visualization

Notation

A	amplitude of vibrating cylinder (m)
D	diameter of cylinder (mm)
f	frequency of vibrating cylinder (Hz)
H	distance between slot end plate and target plate (mm)
h	jet slot width (mm)
Nu	local Nusselt number with cylinder
$\overline{\mathrm{Nu}}$	area-weighed average Nusselt number of Nu
Nu_0	local Nusselt number without cylinder
$\mathrm{Nu}_{0\mathrm{m}}$	arithmetic mean value of local Nusselt numbers without cylinder
$\overline{\mathrm{Nu}}_{0\mathrm{m}}$	area-weighed average Nusselt number $\mathrm{Nu}_{0\mathrm{m}}$
P	static pressure on the surface of flat plate (Pa)
P_0	atmospheric pressure (Pa)
Pt	total pressure at jet exit (Pa)
Q	total electric power (W)
q_c	conduction heat loss per unit area toward the back surface of target plate ($\mathrm{W/m^2}$)
q_net	corrected heat flux ($\mathrm{W/m^2}$)
q_r	radiative heat loss per unit area from strip ($\mathrm{W/m^2}$)
Re	Reynolds number $= U_0 h/\nu$
S	area of heated strip ($\mathrm{m^2}$)
T_b	back surface temperature of target plate (K)
T_w	temperature on the surface of heated strip (K)
T_0	jet temperature (K)
T_∞	ambient room temperature (K)
t	thickness of target plate (mm)
U_0	jet exit velocity (m/s)
V	velocity signal in the wake of cylinder (m/s)
V_cmax	maximum velocity of vibrating cylinder (m/s)
V_mean	time-averaged flow velocity of V (m/s)
v_rms	root mean square values of V (m/s)
X_c	distance between the center of cylinder and target plate (mm)
ε	emissivity of target plate
λ	thermal conductivity (air) (W/m K)
λ_p	thermal conductivity (target plate) (W/m K)
ν	kinematic viscosity ($\mathrm{m^2/s}$)
σ	Stefan–Boltzmann constant ($\mathrm{W/m^2\ K^4}$)

1. Introduction

An impinging jet produces effective heat transfer around the jet stagnation region. Since the jet flow rate and then

* Corresponding author. E-mail: ksuzuki@htrans.mech.kyoto-u.ac.jp.

0142-727X/98/$19.00
PII: S0142-727X(97)10016-9

its heat transfer characteristics can easily be controlled, it is widely used in many practical applications. Sometimes, however, further enhancement of the impinging jet heat transfer is needed. In case of inner surface cooling of high temperature gas turbine vanes, for example, multiple jet impingement is used. The confluence of the injected cooling air from the nozzles inevitably generates a cross flow to each impinging jet. This lowers the stagnation point heat transfer coefficient (Sparrow et al., 1975) and its enhancement is desired. To meet with this demand, a number of works have been reported on the enhancement of impinging jet heat transfer with different means; i.e. (1) insertion of rods (Khan et al., 1980; Kataoka et al., 1991) or a perforated plate (Khan et al., 1982; Kurima et al., 1988), (2) use of an acoustically excited jet (Liu and Sullivan, 1996) or of a pulsed jet Zumbrunnen and Aziz, 1993; Azevedo et al., 1994) to produce flow unsteadiness, and (3) the natural generation of longitudinal vortices with adjusting the direction of jet injection (Nakabe et al., 1997).

The present study treats a new case of combining the above approaches (1) and (2). A cylinder inserted in a space between the jet exit and its target plate was suspended with springs at its both ends. Its mechanically oscillatory motion can be induced in resonance with the vortices shedding from the cylinder itself. This can improve heat transfer in the jet stagnation region where heat transfer is deteriorated by a stagnant recirculating flow region appearing between the mounted cylinder and the target plate. In addition to such an artificial arrangement to enhance the wall heat transfer, another situation is often encountered in practical applications such that some bodies are positioned near heat transfer surface and that they can affect the heat transfer characteristics from the surface. Therefore, studies have been made on how the bodies can affect the surface heat transfer (Marumo et al., 1985; Kawaguchi et al., 1985; Suzuki et al., 1988; Suzuki and Suzuki, 1994; Yao et al., 1995) or on how the surface can affect the heat transfer from bodies (Haneda et al., 1994, 1995a, b. The above kind of interaction between a body inserted in a flow and the vortices shed from the body itself can occur in such occasions depending on how rigidly the body is mounted. Therefore, it should be worthwhile, also from such a general view point, to study how such mechano–fluid interaction can change the heat transfer from a surface located near the body.

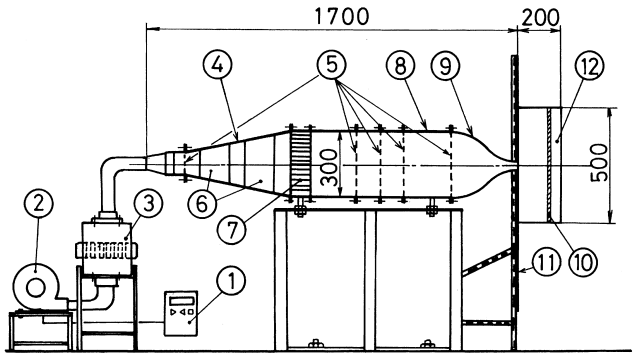

Fig. 1. Experimental apparatus.

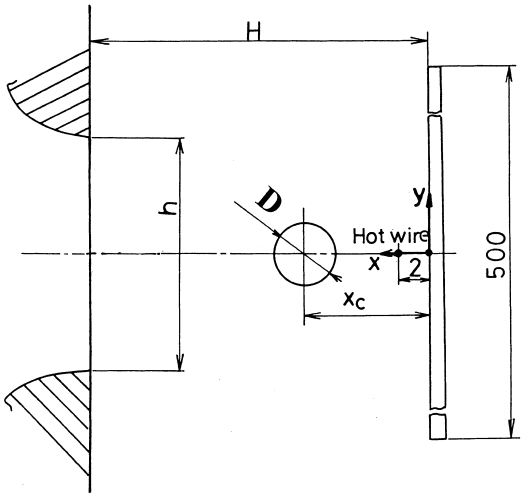

Fig. 2. Coordinate system.

2. Experimental apparatus and procedure

Figs. 1 and 2 show schematic illustrations of the experimental apparatus and the geometry of jet nozzle and target plate system used in the present study. An air jet was discharged from a rectangular slot having the width, h, of 15 mm and the aspect ratio of 33, whose outlet rim was arranged flush mount with the end plate. Two-dimensionality of the impinging jet was secured by mounting two side plates spaced at a distance equal to both the longer side length of the jet slot and the one side width of a target plate. A cylinder was set normal to these side plates in the middle plane of the jet. Two types of cylinders made of aluminium and steel were used and the cylinder diameter was changed in five steps equal to 2, 3, 4, 6 and 8 mm ($D/h = 0.133, 0.2, 0.267, 0.4$ and 0.533). The jet velocity was set at a value so as to keep the jet Reynolds number ranging from 9100 to 10,400. The distance between the slot end plate and the target plate, H, was set equal to $H/h = 3$ and 5, while the distance between the cylinder and the target plate, X_c, was fixed at 8 mm except for one case to be specified as No. 5 below, i.e. $D = 2$ mm and $H/h = 5$, where it was set to be 5 mm. A thin nichrome wire was mounted at the exit of the jet nozzle as illustrated in Fig. 3 to generate smoke in a flow visualization experiments.

Fig. 4 shows the suspension system of the inserted cylinder. The cylinder was suspended by springs at its both ends as illustrated in the figure. Five types of springs tabulated in Table 1 were tested. The tension given to the springs was adjusted by turning the screws attached to one of the springs so as to produce the largest amplitude of cylinder oscillatory motion, which was measured with a ruler. The frequency of the cylinder oscillatory motion was measured from the peak frequency of the power spectrum obtained with Fast Fourier Transform analysis of the velocity and pressure fluctuations respectively detected with a hot-wire anemometer and a pressure transducer. The power spectra of the two signals were established by averaging 256 sets of the FFT analysis data. Experiments were made with nine combinations of different types of cylinder and spring as shown in Table 1.

An I-type hot-wire probe was positioned in the jet middle plane at 2 mm distance from the target plate. The probe was made of a tungsten wire of 5 μm in diameter. For the measurement of pressure fluctuation, a small pressure tap hole of 0.5 mm in diameter was drilled on the target plate at its geometrical center where the origin of the coordinate sys-

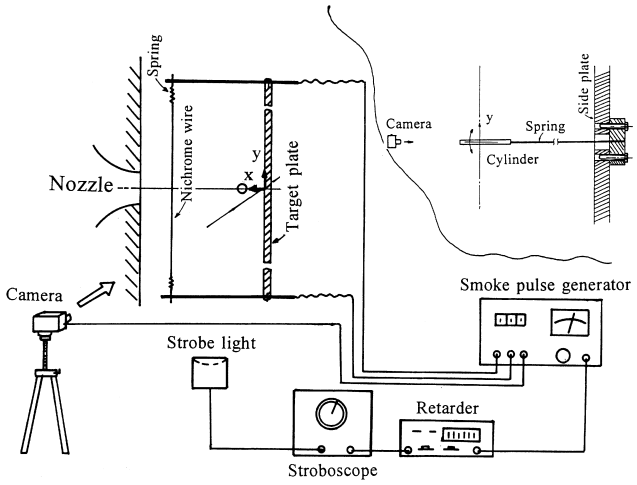

Fig. 3. The method of flow visualization.

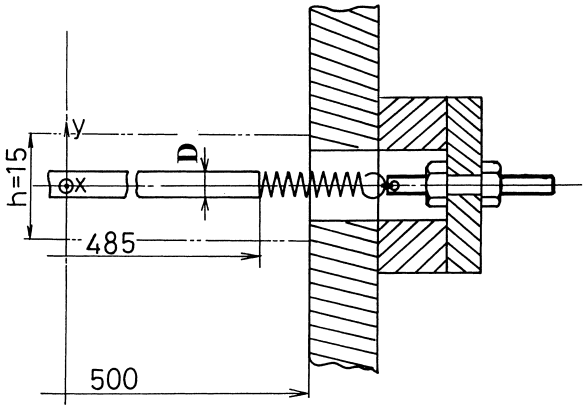

Fig. 4. Detail illustration of the cylinder suspension system.

tem was located. Time variation of the pressure was measured with a pressure transducer connected to the pressure tap. Time mean pressure distribution was measured separately with another target plate on which 61 similar pressure tap holes were also drilled at the spatial interval of 5 mm along the middle of the side plates. The time mean pressure was measured with a manometer connected to these pressure taps.

Seven thin metal strips 20 μm thick and 50 mm wide were glued in parallel with each other to cover the whole target plate surface. These strips were electrically connected in series and were heated by passing alternating electric current. Distribution of the heated surface temperature was measured with 81 thermocouples allocated to contact with the back surface of the central strip at an interval so as to cover the region from $y/h = -15.3$ to $y/h = 15.3$. Heat flux was basically uniform but correction was made for its non-uniformity produced by the radiative heat loss to the ambient and the conduction loss toward the back surface of the target plate. Thus, Nusselt number to be used hereafter was evaluated by the following equation:

$$\mathrm{Nu} = q_{\mathrm{net}} h/\lambda(T_{\mathrm{w}} - T_0),$$

where λ is the fluid thermal conductivity, T_{w} the local heat transfer surface temperature, T_0 the jet temperature and q_{net} is the corrected heat flux and evaluated as follows,

$$q_{\mathrm{net}} = Q/S - q_{\mathrm{r}} - q_{\mathrm{c}},$$

$$q_{\mathrm{r}} = \varepsilon\sigma(T_{\mathrm{w}}^4 - T_{\infty}^4), \qquad q_{\mathrm{c}} = \lambda_{\mathrm{p}}(T_{\mathrm{w}} - T_{\mathrm{b}})/t,$$

where Q is the total electric power input, S the total area of the heated strips, ε the emissivity of the heating surface, σ the Stefan–Boltzmann constant, λ_{p} the thermal conductivity of the target plate having the thickness t, T_{∞} the ambient temperature and T_{b} the back surface temperature of the target plate measured with an additional 23 thermocouples attached to the back surface of the target plate itself. q_{r} and q_{c} were of the order of 2%–5% and 1%–3% of the total heat flux, respectively.

3. Results and discussion

3.1. Flow characteristics

Fig. 5 shows the long time exposure photograph of the oscillating cylinder. The amplitude of y-direction motion

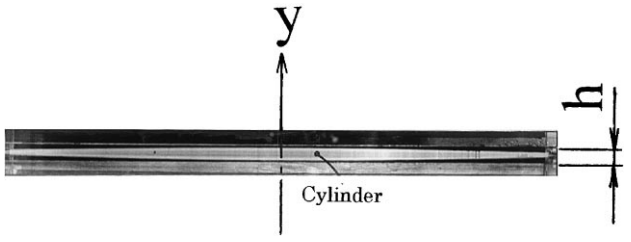

Fig. 5. Photograph of an oscillating cylinder.

Table 1
Dimensions of several springs and characteristic of cylinder oscillation

Spring number	Diam. of cylinder (mm)	Material of cyl. pipe	Diam. of wire (mm)	Outer diam. of spring (mm)	Free length of spring (mm)	2·Amplitude (mm)		Frequency (Hz)	
						$H/h = 3$	$H/h = 5$	$H/h = 3$	$H/h = 5$
No. 1	4	Aluminum	0.25	3.2	12	8	7	27	28
No. 2	4	Aluminum	0.40	4.0	10	2	3	29	31
No. 3	4	Aluminum	0.29	2.5	9	3	7	25	25
No. 4	4	Aluminum	0.50	4.0	12	3	7	37.5	37.5
No. 5	2	Steel	0.20	2.0	14	2	5	13.5	13
No. 6	3	Aluminum	0.40	4.0	6	4	3	32.5	31.5
No. 7	3	Steel	0.29	2.5	10	2	3	25	23.5
No. 8	6	Aluminum	0.50	4.0	9	4	6	43	43
No. 9	8	Aluminum	0.40	4.0	10	2	–	28	–

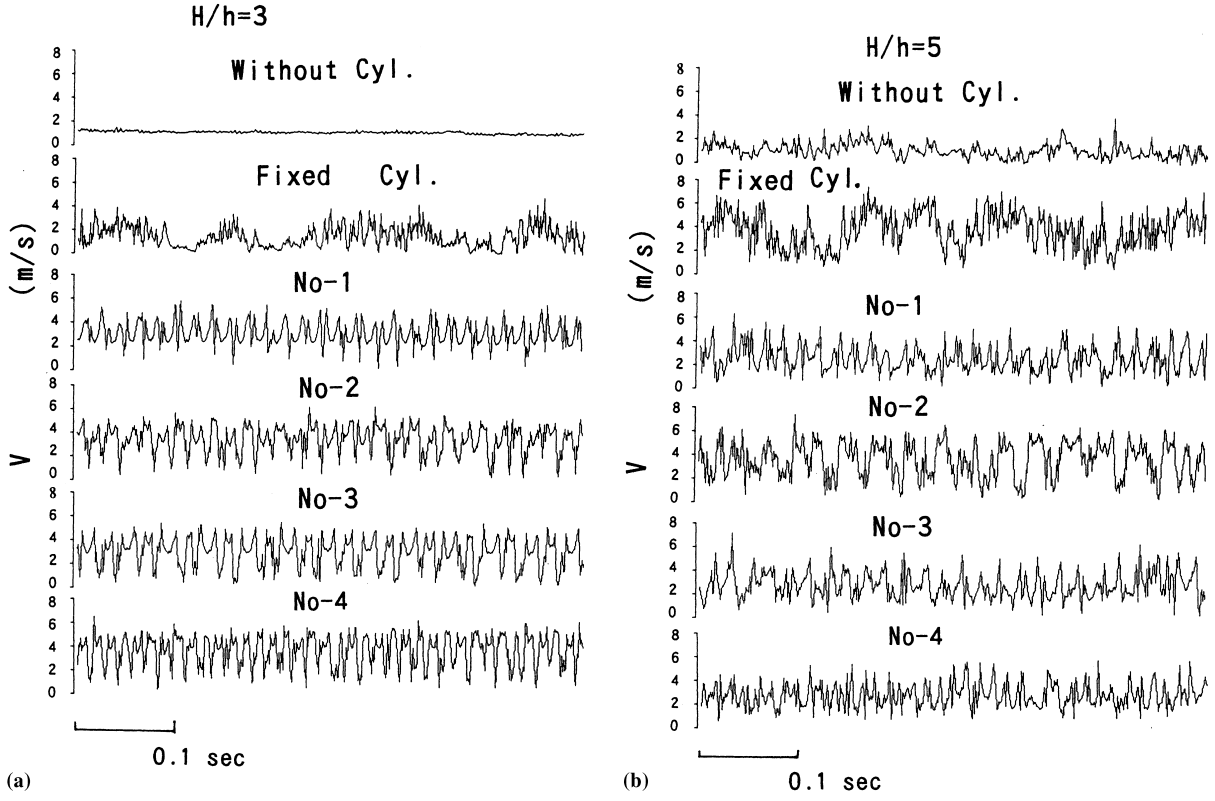

Fig. 6. Time traces of velocity near the flat plate.

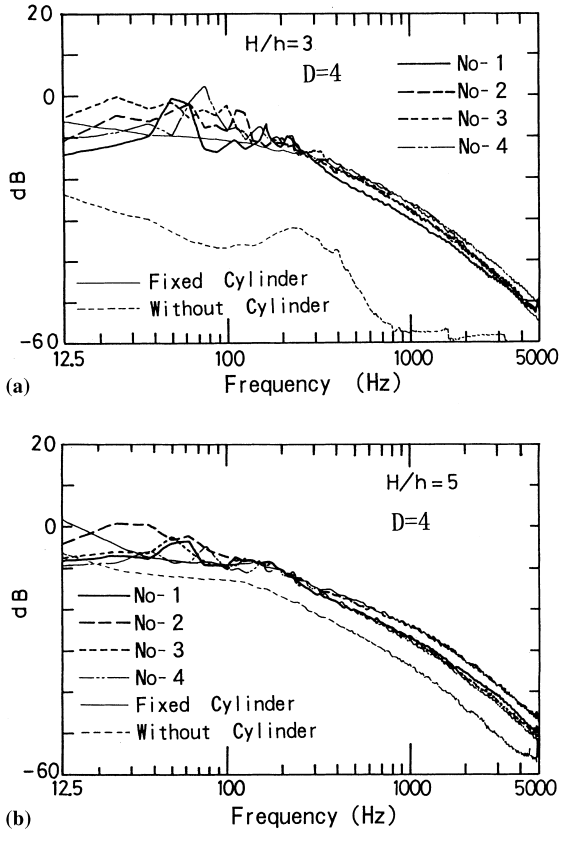

Fig. 7. Power spectrum distributions of fluctuating velocity near the flat plate.

of the cylinder is almost uniform along the cylinder axis. Thus, the observed oscillation is caused by the deformation of the springs attached to the ends of the cylinder. The elasticity of the cylinder itself contributes little to its oscillation.

Fig. 6(a) and (b) shows the time trace of the velocity obtained respectively when H/h was set equal to 3 and 5. In the case where no cylinder was inserted, the velocity signal is very smooth in Fig. 6(a) suggesting that the flow approaching the target plate must have remained laminar. When $H/h = 5$ (Fig. 6(b)), the velocity signal shows irregularity indicating that the impinging distance was long enough for the laminar to turbulent transition to occur in the jet middle plane. However, the velocity signal shows much more conspicuous fluctuation when the cylinder was inserted. In particular, in all the illustrated cases No. 1–4 where mechanical oscillation of the cylinder was introduced, periodicity of velocity fluctuation became more pronounced indicating that the flow approaching to the target plate was modified by the introduced mechanical

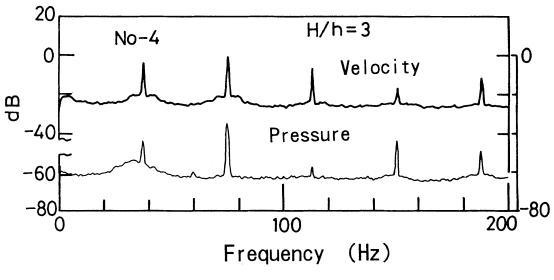

Fig. 8. Spectral distributions of velocity and pressure fluctuations on the surface of the flat plate behind cylinder.

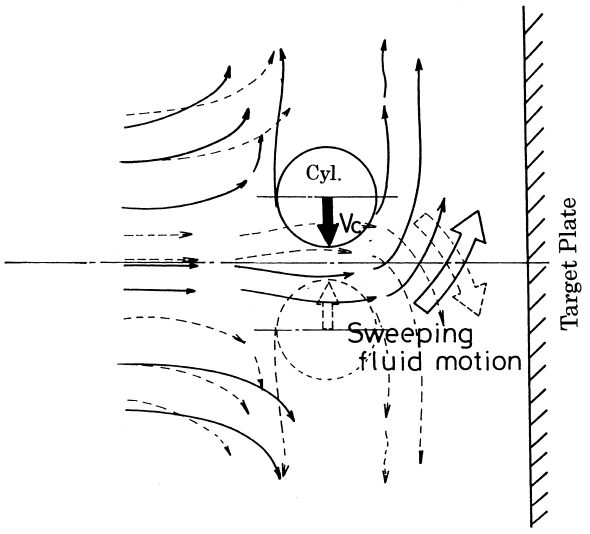

Fig. 9. Schematic flow pattern.

oscillation of the cylinder. The frequency of velocity oscillation is observed to clearly vary with the change in the used spring constant.

What was just discussed can be confirmed again in Fig. 7(a) and (b) in which the power spectra of the velocity fluctuations are shown. The spectrum for the normal impinging jet case without insertion of a cylinder is distinctly lower in all frequency range as is observed in Fig. 7(b) for $H/h = 5$ than the counterparts of the cases where the cylinder was inserted. The lower profile of the normal impinging jet spectrum is much more pronounced in Fig. 7(a) for $H/h = 3$. In every case where the spring-suspended cylinder was used, a peaky profile becomes noticeable in the velocity fluctuation spectrum in the frequency range less than 100 Hz indicating the generation of periodical velocity fluctuation. This is observed in a much more pronounced manner in Fig. 8 in which the spectrum is plotted against the frequency of normal scale. The lowest peaky frequency detected in the spectrum was included in the right column of Table 1.

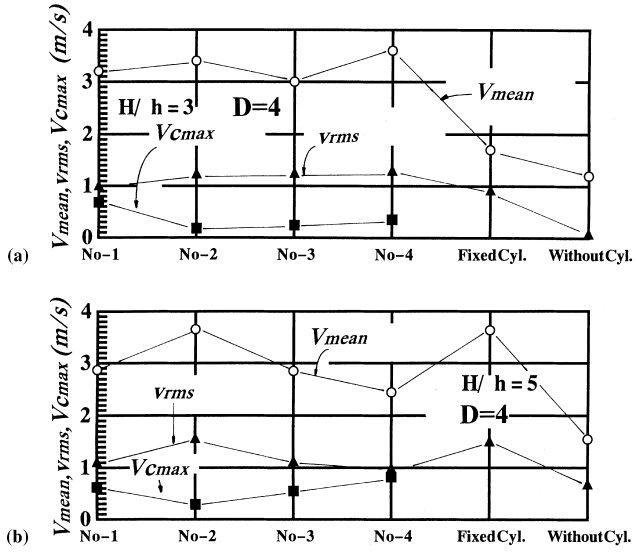

Fig. 10. Relations between velocities and conditions for 4 mm cylinder diameter.

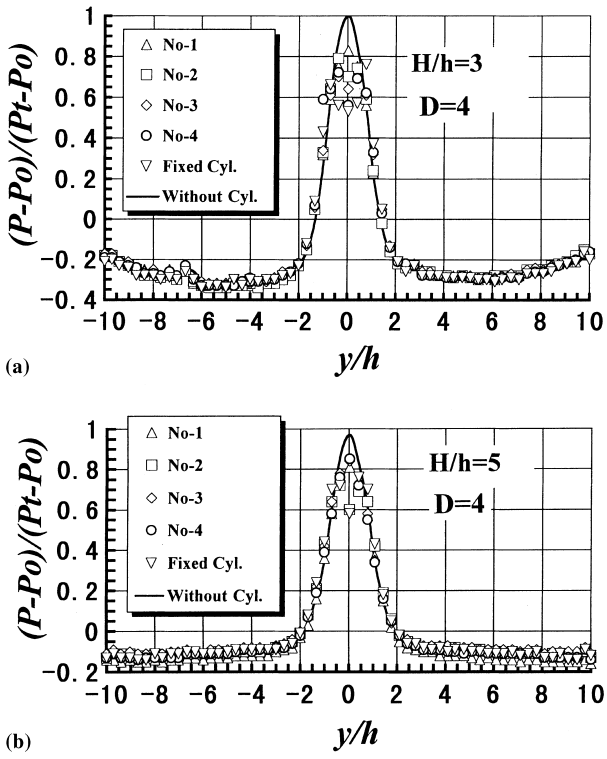

Fig. 11. Distributions of mean pressure on the flat plate for 4 mm cylinder diameter.

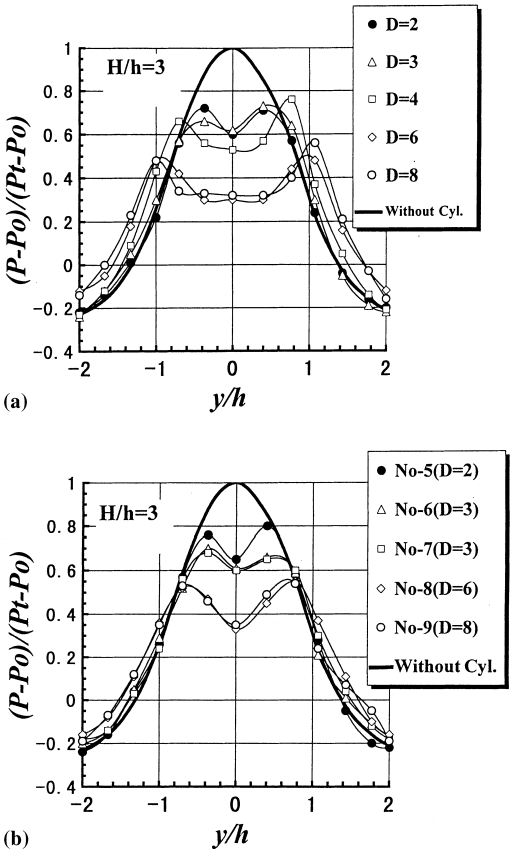

Fig. 12. Distributions of mean pressure on the flat plate at $H/h = 3$ for different cylinder diameters.

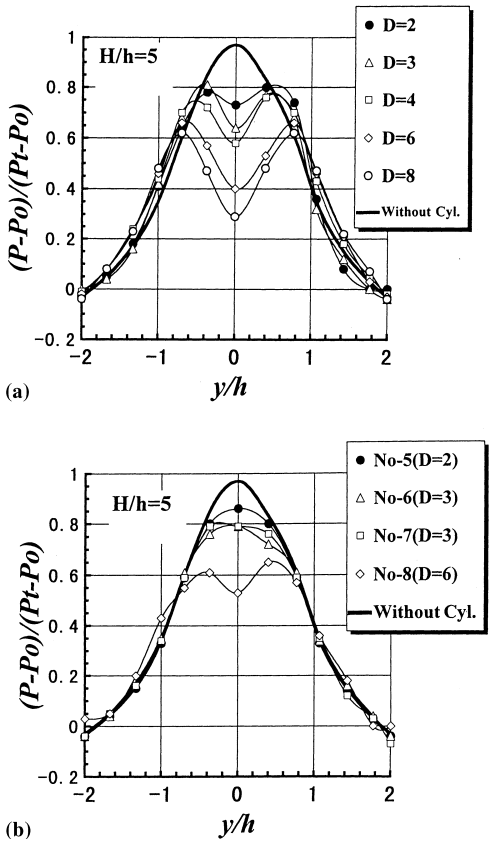

Fig. 13. Distributions of mean pressure on the flat plate at $H/h = 5$ for different cylinder diameters.

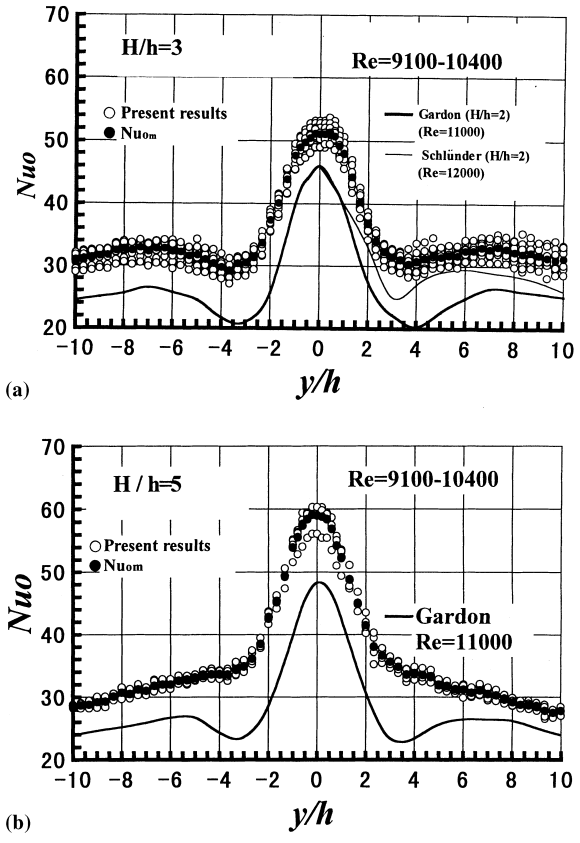

Fig. 15. Distributions of local Nusselt number for normal impinging jet.

One more thing worth to note in Fig. 8 is that the spectrum of the pressure fluctuation detected on the target plate surface has a peak as well and in particular at the same frequency as that of the velocity fluctuation. A conjecture can be developed from these results that the velocity field fluctuation, at least, around the stagnation region should have been a swing-type one; fluid sweeps the target plate stagnation region in the y-positive direction in half cycle and in the opposite direction in another half cycle. In Fig. 9 is illustrated a conceptual schematic of the swing-type flow fluctuation; solid lines show that in one half cycle when flow is directed towards the positive y-direction and dotted lines that in another half cycle when flow is directed in the opposite direction. This type of swinging flow will be induced by a slight

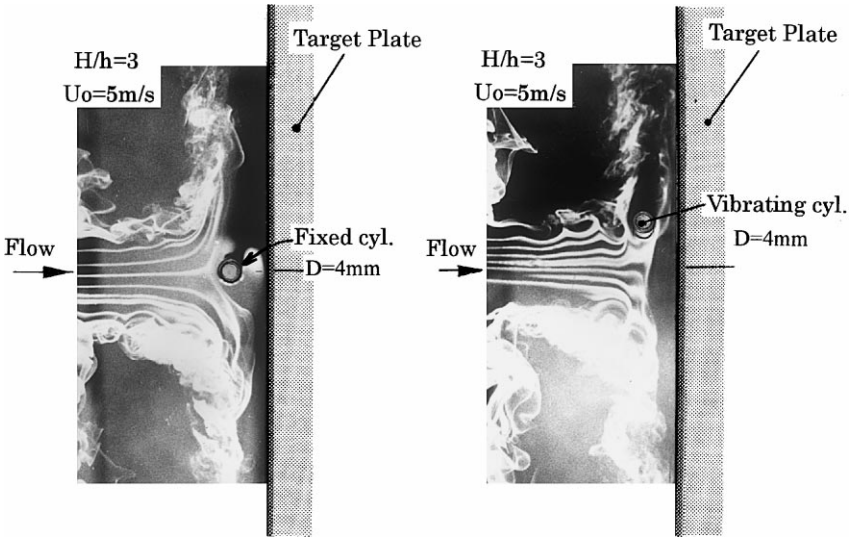

Fig. 14. Photographs of flow visualization by smoke wire method.

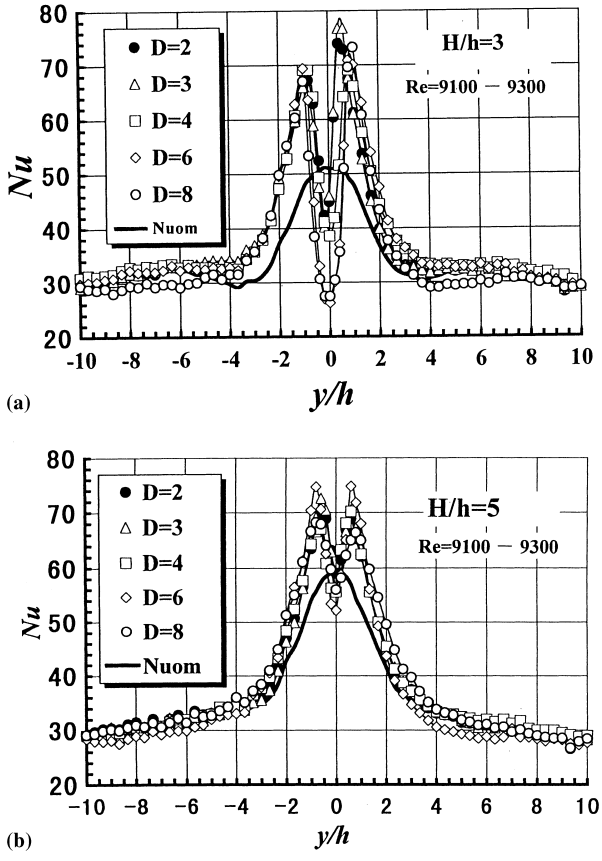

Fig. 16. Distributions of local Nusselt number in the cases of mounting stationary cylinder.

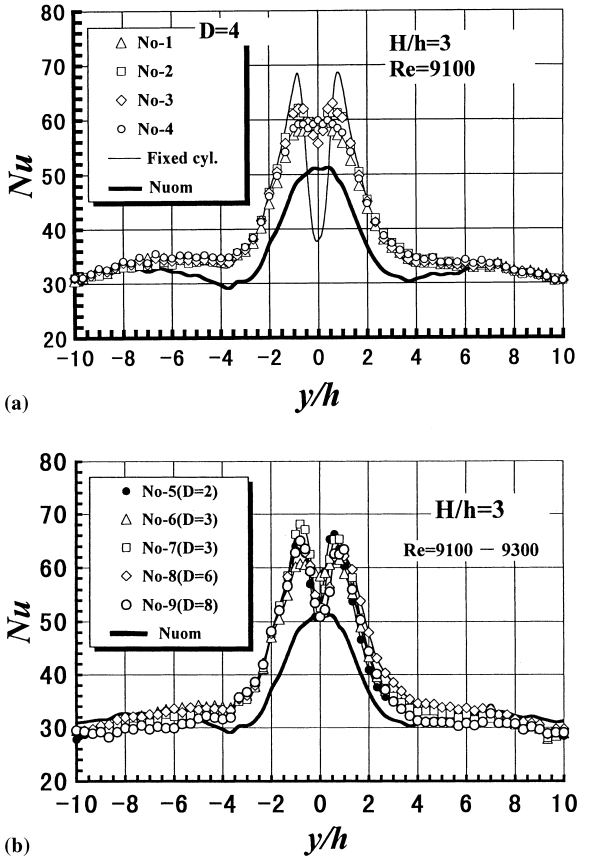

Fig. 17. Distributions of local Nusselt number at $H/h = 3$ in the cases of mounting oscillatory cylinder.

asymmetry of the system caused by the cylinder oscillatory motion and by the interaction with the asymmetric shedding of vortices behind the cylinder.

Fig. 10(a) and (b) shows the time-averaged velocity, V_{mean}, the root mean square value of velocity fluctuation, v_{rms}, and the maximum cylinder displacement velocity, V_{cmax}, for one case of the normal impinging jet, another case with the rigidly suspended cylinder and four other cases with the spring-suspended cylinder No. 1–4. V_{cmax} was evaluated as being equal to $2\pi fA$ where f is the frequency tabulated in Table 1, and A the cylinder displacement amplitude measured from the photographs like the one shown in Fig. 5. The value of v_{rms} is much larger than V_{cmax} in all the cases indicating not that the velocity fluctuation is generated by the motion of the cylinder but that, as is conjectured in the above, it is induced in the cylinder wake, particularly in the case with the spring-suspended cylinder, by the asymmetric position of the cylinder and by the interaction with the modified shedding of vortices from the cylinder. V_{mean} as well as v_{rms} increases in the cases with the spring-suspended cylinder and it is twice larger than v_{rms}. This supports a speculation developed above such that the flow fluctuation around the stagnation region is a swing-type one.

The distribution of mean pressure measured on the target plate is plotted in Fig. 11(a) and (b). P is the local value of pressure measured on the target plate, P_0 an atmospheric pressure, and Pt the total pressure measured at the jet exit. In all the cases with the cylinder, pressure is conspicuously lower around the stagnation region than its counterpart of the normal impinging jet without an insertion of cylinder. Especially in the case with the rigidly suspended cylinder, local minimum appears at the center of the target plate suggesting the appearance of a recirculating flow region. However, pressure at the geometrical stagnation point is larger in the cases with the spring-suspended cylinder than in the case of rigidly suspended cylinder and pressure of the cases with an insertion of spring-suspended cylinder is larger outside the stagnation region compared to the counterpart of normal impinging jet. This is more clearly confirmed in Figs. 12 and 13 in which pressure distribution near the jet middle plane was closed up. The pressure distribution just discussed again supports the speculation that the flow field is fluctuating in a swing-type manner in those cases. One more thing to be noted here is that, in the skirt of the impinging jet, pressure is lower than the atmospheric one. This suggests a possibility that a weak recirculating flow might have been generated between the end plate and the target plate. In this sense, the studied impinging jet may not be of a complete open flow system.

Fig. 14 shows two photographs taken in the flow visualization experiments, for the case where the rigidly suspended cylinder was inserted and for another case where the spring-suspended cylinder was mounted. In the latter case, fluid is observed to flow around the cylinder displaced to a position off the jet middle plane and to sweep the target plate. This agrees with the above developed conjecture about a possible swing-type flow near the target plate.

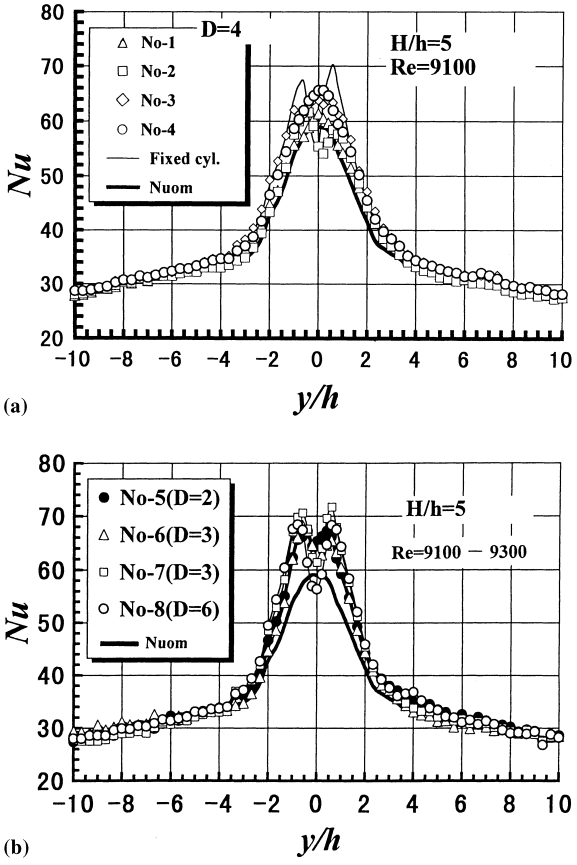

Fig. 18. Distributions of local Nusselt number at $H/h = 5$ in the cases of mounting oscillatory cylinder.

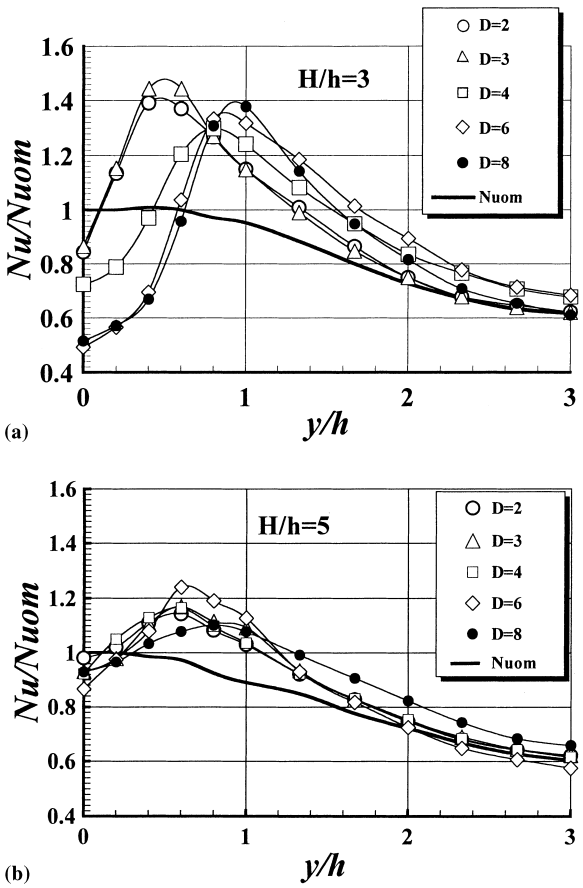

Fig. 19. Distributions of local Nusselt number normalized by $\overline{\mathrm{Nu}}_{0m}$ in the cases of mounting stationary cylinder.

3.2. Heat transfer characteristics

Reproducibility of heat transfer data was studied for the normal impinging jet case. All the heat transfer data obtained in eleven times repeats of the measurement for the case of $H/h = 3$ and five times of the measurement for the case of $H/h = 5$ are respectively plotted in the form of the Nusselt number, Nu_0, in Fig. 15(a) and (b). Standard deviation of Nu_0 was 4.5% and 3.6% at maximum for respective cases.

Solid symbols plotted in the both figures show the averaged value of the presently measured data. They are distinctly higher than the results reported by Gardon and Akfirat (1966) and Schlunder et al. (1970). This discrepancy may have resulted from the difference in the shape and size of the nozzle between their experiments and the present one. In the case of an axisymmetric impinging jet, the shape of the nozzle can affect the heat transfer data seriously and detailed experiments on this are under progress at Kyoto University. San et al. (1997) recently reported for an axi-symmetric impinging jet that Nusselt number decreased with the decrease in the size of the nozzle. The development pattern of turbulence along the jet axis reported by Gardon and Akfirat for smaller size nozzle was different from the present one measured in the preliminary study.

Fig. 16(a) and (b) presents the measured Nusselt number, Nu, for the cases with the insertion of rigidly suspended cylinder. As is observed in these figures, by the insertion of rigidly suspended cylinder, effective heat transfer enhancement can be achieved at the rim of the stagnation region by almost 40% and more than 20% respectively for $H/h = 3$ and $H/h = 5$. However, around $v/h = 0$, the center of the target plate, occurrence of significant deterioration of heat transfer is observed. This should be produced by the stagnant flow in that region.

Figs. 17 and 18 show the heat transfer data obtained for all the cases No. 1–9 where the cylinder suspended with different types of springs was used. In the figures, similar data obtain for the normal case of impinging jet without an insertion of cylinder and for the cases with the insertion of a rigidly suspended cylinder. The same data are replotted in Figs. 19 and 20 in the form normalized with the peak value Nu_{0m} obtained at the stagnation point $y/h = 0$ for the normal impinging jet case without an insertion of cylinder. In almost all of the cases with the insertion of the spring suspended, the largest enhancement ratio of heat transfer is a little lower than in the case with a rigidly suspended cylinder and it is about 25% at most. However, enhancement can be obtained uniformly over the whole studied range of position except for one or two exceptional cases. A significant local minimum appears in the profile of the pressure distribution in such cases, as is found in Figs. 12 and 13, in an almost similar fashion with the one for the case with the rigidly suspended cylinder. In all other cases, heat transfer deterioration no more occurs around $y/h = 0$, the center of the target plate, while a slight local minimum still exists in the profile Nu in some cases. This enhancement should have

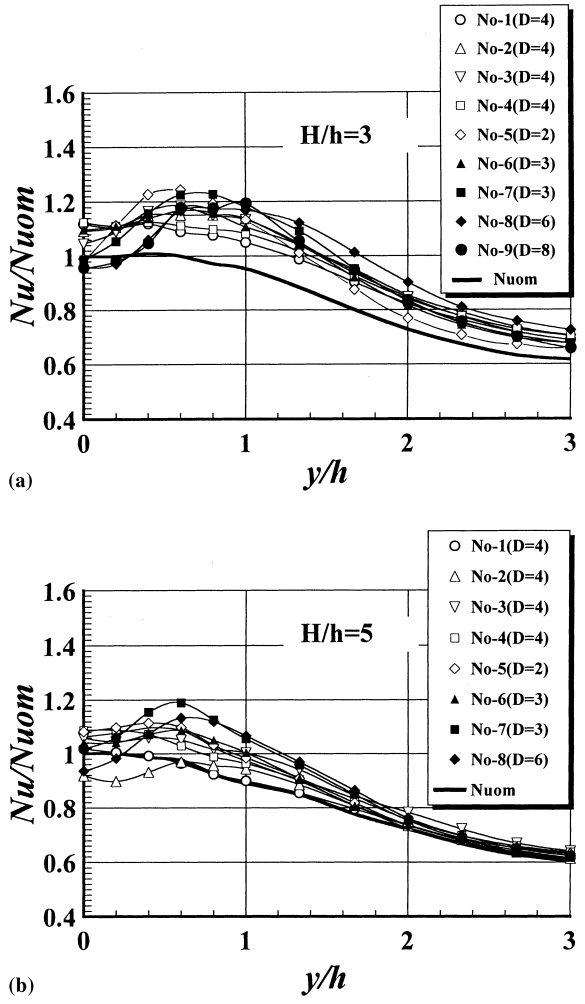

Fig. 20. Distributions of local Nusselt number normalized by $\overline{Nu}_{0m}$ in the cases of mounting oscillatory cylinder.

been attained by the sweep of heated fluid by the generated swing-type pattern of flow fluctuation discussed above.

As is observed in Fig. 21, 10% enhancement of spatial mean heat transfer averaged over the region $-10 \leqslant y/h \leqslant 10$ can be achieved in the case where $H/h = 3$. The enhancement ratio is almost the same in level both for the cases with the insertion of rigidly suspended cylinder and with the insertion of the spring-suspended cylinder.

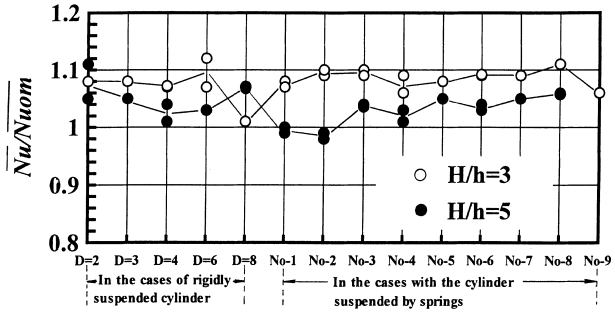

Fig. 21. Enhancement of spatial mean Nusselt number ($-10 \leqslant y/h \leqslant 10$).

However, when $H/h = 5$, the enhancement of space mean Nusselt number to be attained with the insertion of the spring-suspended cylinder is almost nothing for the cases No. 1 and No. 2. In other cases of $H/h = 5$, the insertion of a cylinder suspended with springs enhances the space mean Nusselt number by about 5%, again being the same in level as for the cases with the insertion of a rigidly suspended cylinder. Thus, the usage of the spring-suspended cylinder is not effective to improve the space mean Nusselt number but effective just to improve the local heat transfer around the stagnation region.

4. Conclusions

Possibility of enhancement of two-dimensional impinging jet heat transfer was studied experimentally. In particular, the effectiveness of mechano–fluid interactive flow oscillation induced by making use of a cylinder suspended with springs was studied. Cross-stream periodical motion of the cylinder was induced in this case. With the insertion of such a cylinder, the power spectrum of velocity fluctuation detected just above the center of the target plate was observed to be higher in the low frequency range below 200 Hz and to be characterized by peaky profile suggesting the generation of periodical velocity fluctuation. At the same time, mean velocity and velocity fluctuation intensity was confirmed to be brought higher. These suggested the generation of swing-type flow field fluctuation and such a type of flow oscillation was actually confirmed to exist through flow visualization. This flow modification enhances the local heat transfer around the jet stagnation region and the local Nusselt number becomes almost uniform over the stagnation region on the target plate. The enhancement ratio of the space mean Nusselt number is about 10% and is almost equal to the one attained with the insertion of rigidly suspended cylinder. Effectiveness of heat transfer enhancement was higher when the target plate was located at the distance from the jet exit of three times the jet slot width.

References

Azevedo, L.F.A., Webb, B.W., QuEeiroz, M., 1994. Pulsed air jet impingement heat transfer. Experimental Thermal and Fluid Science 8, 206–213.

Gardon, R., Akfirat, J.C., 1966. Heat transfer characteristics of impinging two-dimensional air jet. Trans. ASME: J. Heat Transfer 88, 101–108.

Haneda, Y., Tsuchiya, Y., Kurasawa, H., Suzuki, K., 1994. A study on the two-dimensional jet impinging on a circular cylinder (1st report, measurements of flow-field and heat transfer around a circular cylinder mounted near two flat plate). Trans. JSME 60-572B, 1401–1407 (in Japanese).

Haneda, Y., Tsuchiya, Y., Kurasawa, H., Suzuki, K., 1995a. A two-dimensional jet impinging heat transfer on a circular cylinder (2nd report, effect of angles between two plates mounted near the cylinder). Trans. JSME 61-583B, 1078–1084 (in Japanese).

Haneda, Y., Tsuchiya, Y., Kurasawa, H., Suzuki, K., 1995b. Impinging jet heat transfer from a circular cylinder mounted in a converging channel between inclined plates. Proceedings of the Sixth Asian Congress of Fluid Mechanics, vol. II, pp. 939–942.

Kataoka, K., Ohmura, N., Hamano, S., 1991. Heat transfer augmentation by combination of jet flow with wake flow. Proceedings of the 28th National Heat Transfer Symposium of Japan. pp. 70–72 (in Japanese).

Kawaguchi, Y., Suzuki, K., Sato, T., 1985. Heat transfer promotion with a cylinder array located near the wall. Internat. J. Heat and Fluid Flow 6 (4), 249–255.

Khan, M.M.A., Kasagi, N., Hirata, M., Nisiwaki, N., 1982. Heat transfer augmentation in an axisymmetric impinging jet. Proc. Seventh Internat. Heat transfer Conf. 3, 363–368.

Khan, M.M.A., Ohnishi, H., Kasagi, N., Hirata, M., Kawabata, J., 1980. Technic of heat transfer augmentation in an axisymmetric impinging jet (3rd report). Proceedings of the 17th National Heat Transfer Symposium of Japan, pp. 40–42 (in Japanese).

Kurima, J., Miyamoto, M., Harada, T., 1988. Heat transfer augmentation of axisymmetric impinging jet using a perforated plate set in front of a target plate (1st report, the effects of diameter and pitch of holes in a perforated plate). Trans. JSME 54-503B, 1736–1743 (in Japanese).

Liu, T., Sullivan, J.P., 1996. Heat transfer and flow structures in an excited circular impinging jet. Internat. J. Heat Mass Transfer 39 (17), 3695–3706.

Marumo, E. Suzuki, K., Sato, T., 1985. Turbulent heat transfer in a flat plate boundary layer disturbed by a cylinder. Internat. J. Heat and Fluid Flow 6 (4), 241–248.

Nakabe, K., Inaoka, K., Ai, T., Suzuki, K., 1997. An experimental study on flow and heat transfer characteristics of longitudinal vortices induced by an inclined impinging jet in a crossflow. Proc. Third KSME-JSME Thermal Engrg. Conf. III, 59–64.

San, J., Huang, C., Shu, M., 1997. Impingement cooling of a confined circular air jet. Internat. J. Heat Mass Transfer 40 (6), 1355–1364.

Schlunder, E.U., Krotzsch, P., Hennecke, F.W., 1970. Gesetzmasigkeiten der Warme-und Stoffubertragung bei der Prallstromung aus Rund-und Schlitzdusen. Chem.-Ing.-Tech. 42 (6), 333–338.

Sparrow, E.M., Goldstein, R.J., Rouf, M.A., 1975. Effect of nozzle-surface separation distance on impingement heat transfer for a jet in a crossflow. Trans. ASME: J. Heat Transfer 97, 528–533.

Suzuki, H., Suzuki, K., Sato, T., 1988. Dissimilarity between heat and momentum transfer in a turbulent boundary layer disturbed by a cylinder. Internat. J. Heat Mass Transfer 31 (2), 259–265.

Suzuki, K., Suzuki, H., 1994. Unsteady heat transfer in a channel obstructed by an immersed body. Ann. Rev. Heat Transfer 5, 177–206.

Yao, M., Nakatani, M., Suzuki, K., 1995. Flow visualization and heat transfer experiments in a turbulent channel flow obstructed with an inserted square rod. Internat. J. Heat and Fluid Flow 16, 389–397.

Zumbrunnen, D.A., Aziz, M., 1993. Convective heat transfer enhancement due to intermittency in an impinging jet. Trans. ASME: J. Heat Transfer 115, 91–98.